Supplement of Atmos. Chem. Phys., 26, 16545–16570, 2026
https://doi.org/10.5194/acp-26-16545-2026-supplement
© Author(s) 2026. CC BY 4.0 License.



Atmospheric Chemistry and Physics
Open Access
EGU

Supplement of

Saharan dust transport and boundary layer entrainment over western Europe: multi-instrument observations and convection-permitting model evaluation

Hengheng Zhang et al.

Correspondence to: Hengheng Zhang (zhang@riam.kyushu-u.ac.jp) and Harald Saathoff (harald.saathoff@kit.edu)

The copyright of individual parts of the supplement might differ from the article licence.

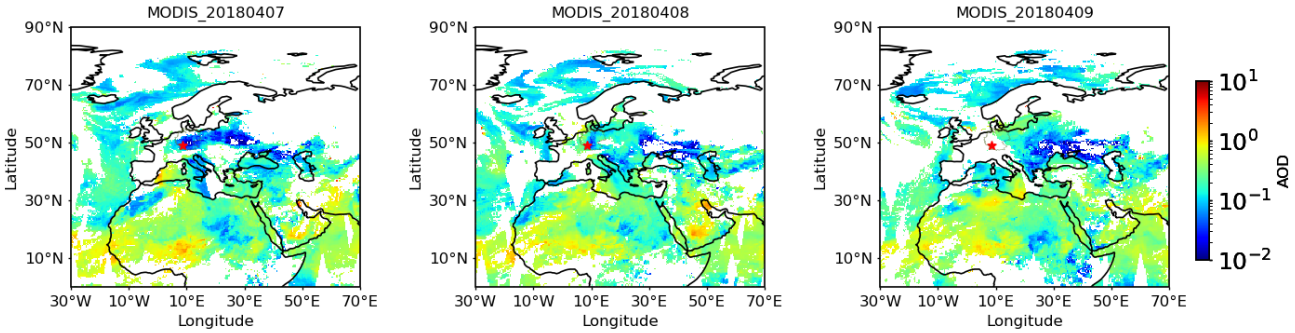


Figure S1. Horizontal maps of daily averaged aerosol optical depth (AOD) from MODIS retrieval and CAMS dataset with spatial resolution of $0.4^\circ * 0.4^\circ$ from April 7^{th} to 9^{th}, 2018 for case 1.

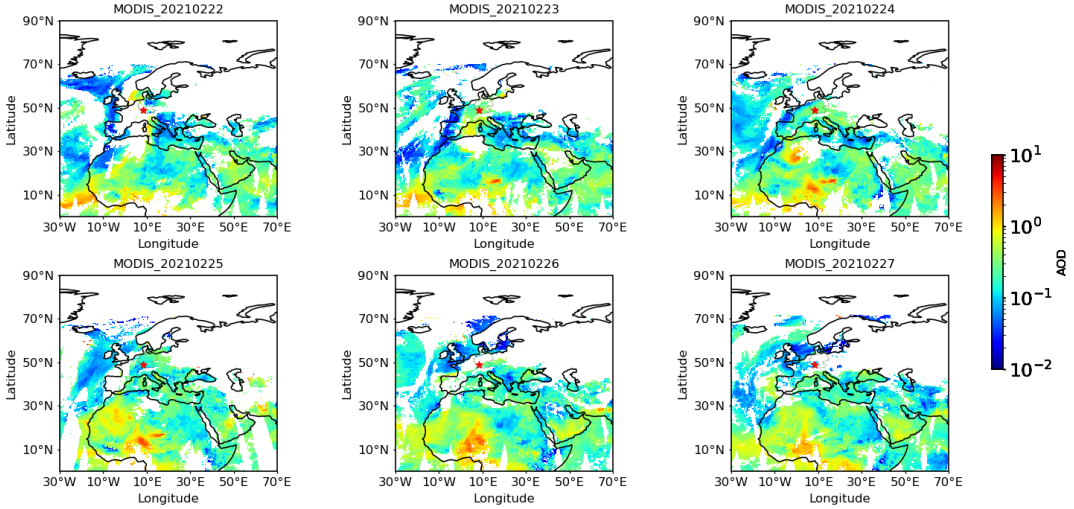


Figure S2. Horizontal maps of daily averaged aerosol optical depth (AOD) from MODIS retrieval and CAMS dataset with spatial resolution of $0.4^\circ * 0.4^\circ$ from February 22^{th} to 26^{th}, 2021 for case 2.

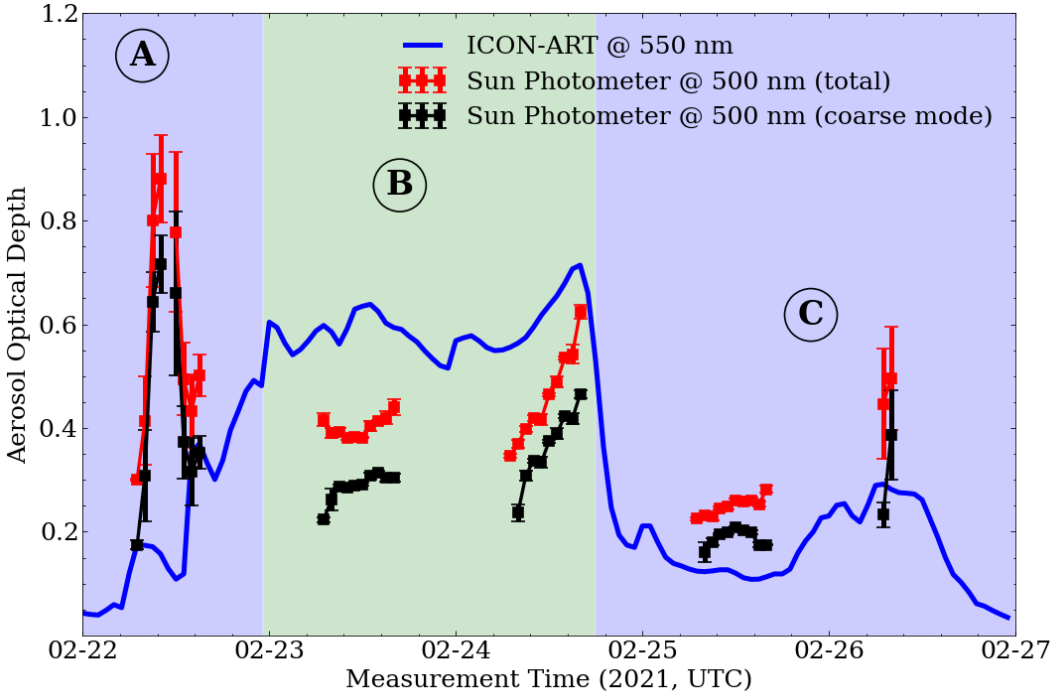


Figure S3. Case 2 time series of AODs from the sun photometer at 500 nm and ICON-ART model simulations at 550 nm between 22^{nd} and 26^{th} February 2021 for 1-hour temporal resolution.

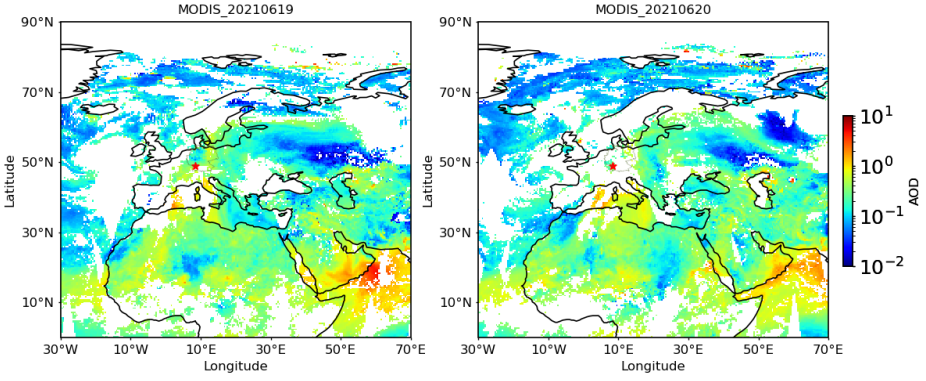


Figure S4. Horizontal maps of daily averaged aerosol optical depth (AOD) from MODIS retrieval and CAMS dataset with spatial resolution of $0.4^{\circ} * 0.4^{\circ}$ from June 19^{th} to 20^{th}, 2021 for case 3.

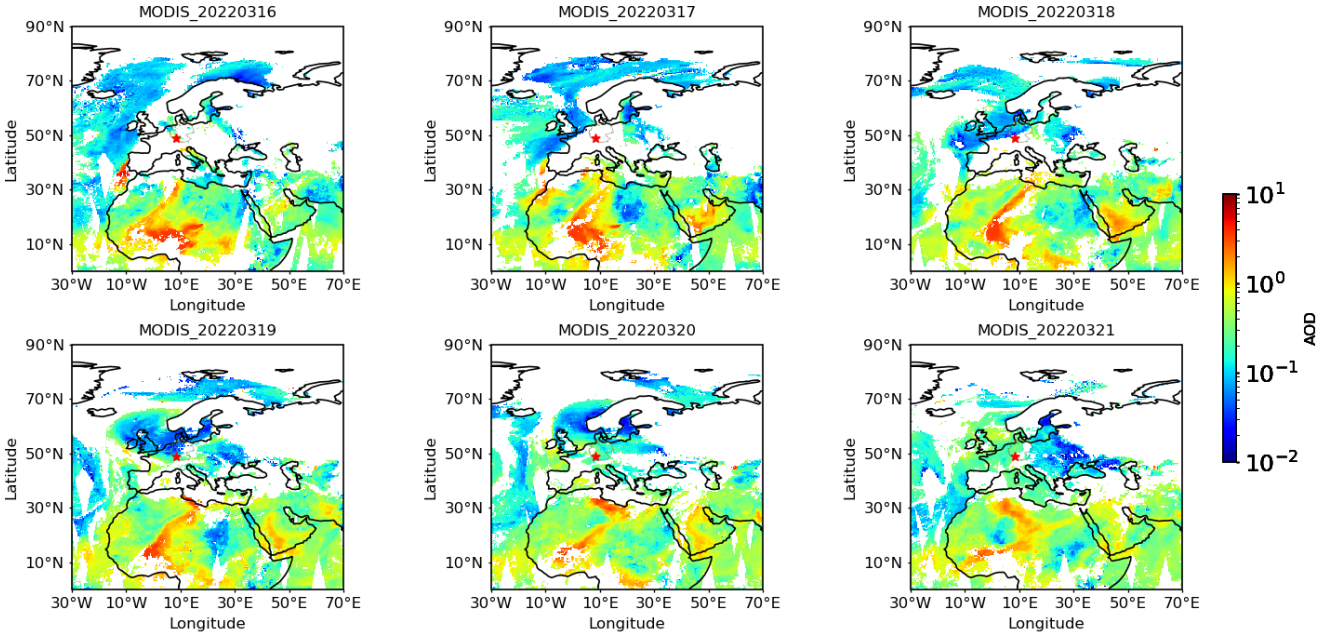


Figure S5. Horizontal maps of daily averaged aerosol optical depth (AOD) from MODIS retrieval and CAMS dataset with spatial resolution of $0.4^{\circ} * 0.4^{\circ}$ from March 17^{th} to 22^{th}, 2022 for case 4.

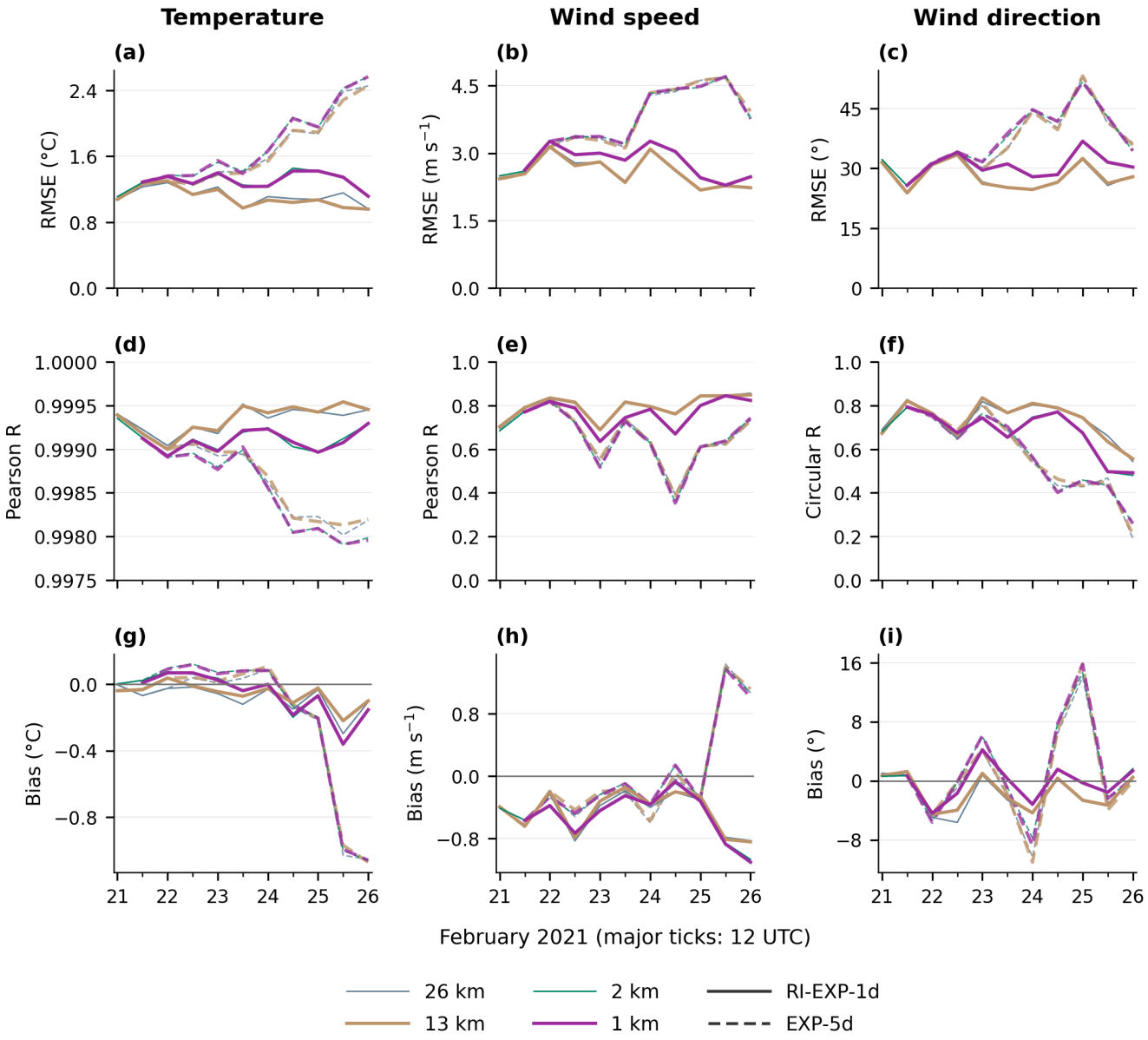


Figure S6. Time series of station-mean full-column RMSE (a–c), correlation coefficient R (d–f), and bias (g–i) for temperature (left column), wind speed (middle column), and wind direction (right column), from 21 February 2021 at 12:00 UTC to 26 February 2021 at 12:00 UTC.

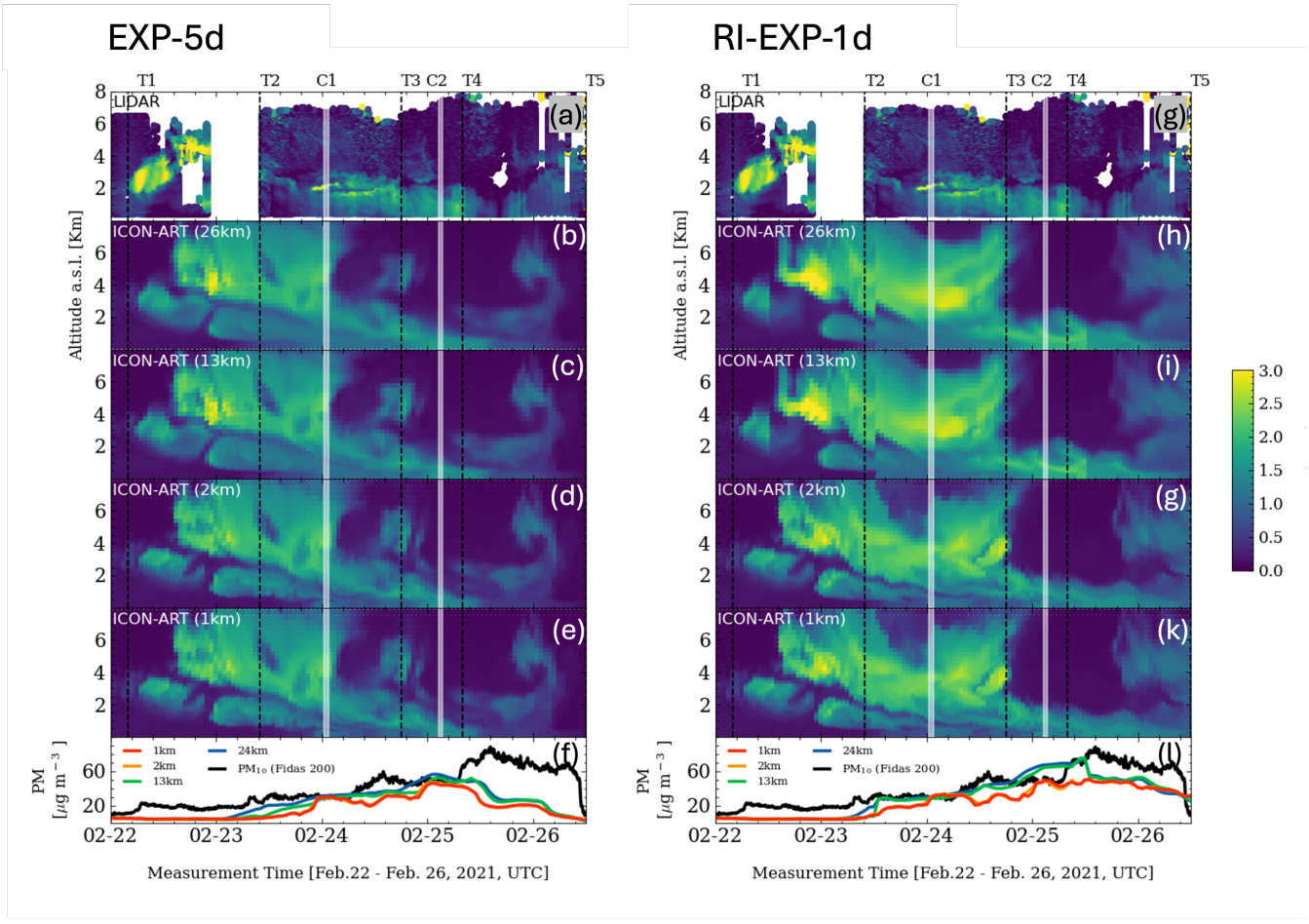


Figure S7. Time–height cross section of lidar backscatter coefficient(a). Corresponding ICON-ART backscatter coefficient simulated at horizontal grid spacings of 26 km, 13 km, 2 km, and 1 km, respectively(b–e). Time series of surface PM concentration measured by Fidas 200 (black) and simulated by ICON-ART (f) from 22^{nd} to 26^{th} February 2021. Panels (h-l) are the same as panels (b–f), but for the RI-EXP-1d experiment.

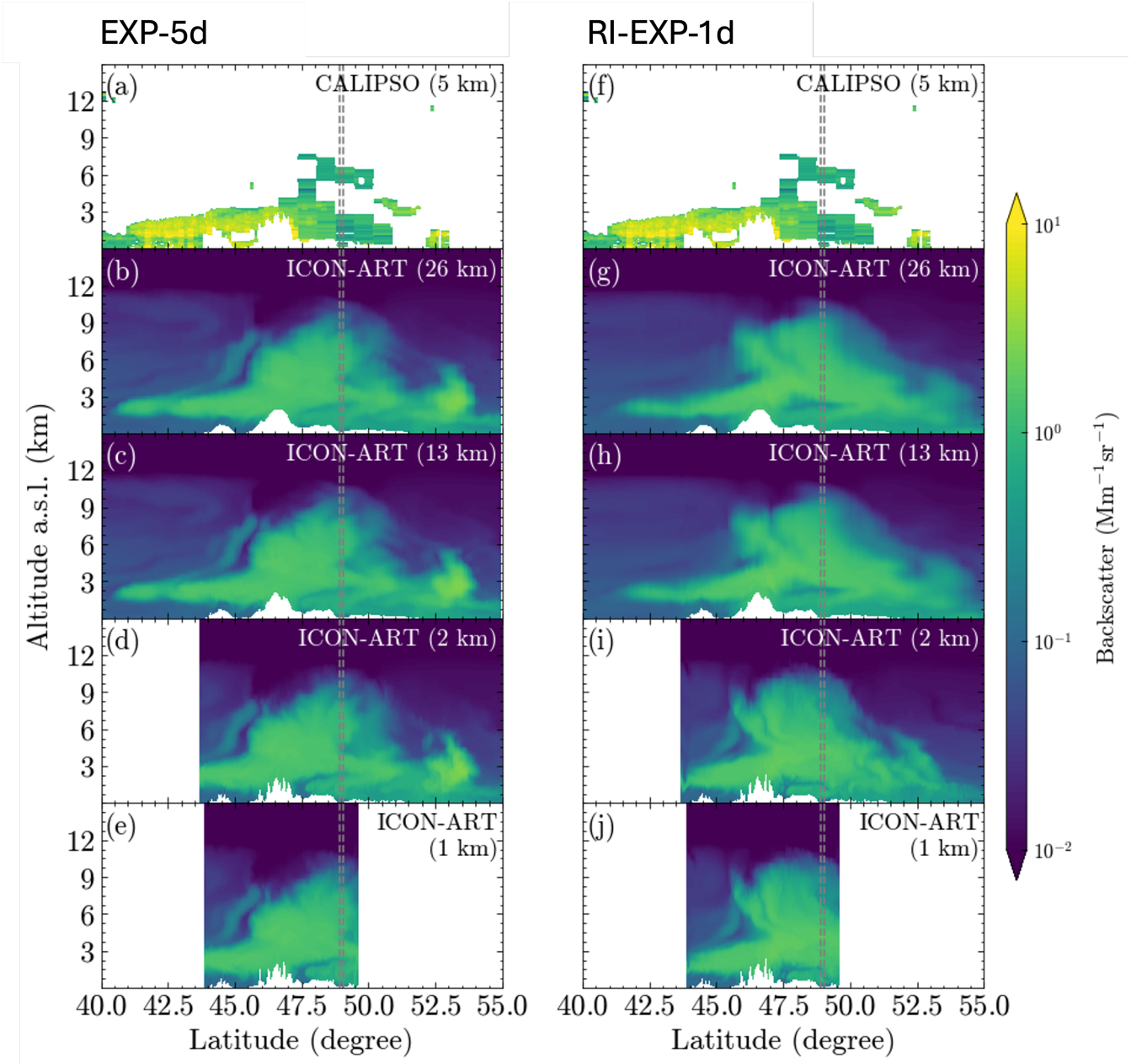


Figure S8. Latitude height of backscatter coefficient at 532 nm from CALIPSO retrieval (a) and ICON-ART simulation for horizontal grid spacings from 26 km to 1 km, respectively(b–e). Panels (g-j) are the same as panels (b–g), but for the RI-EXP-1d experiment. The data was sampled at 13:00 UTC on 23 February 2021.

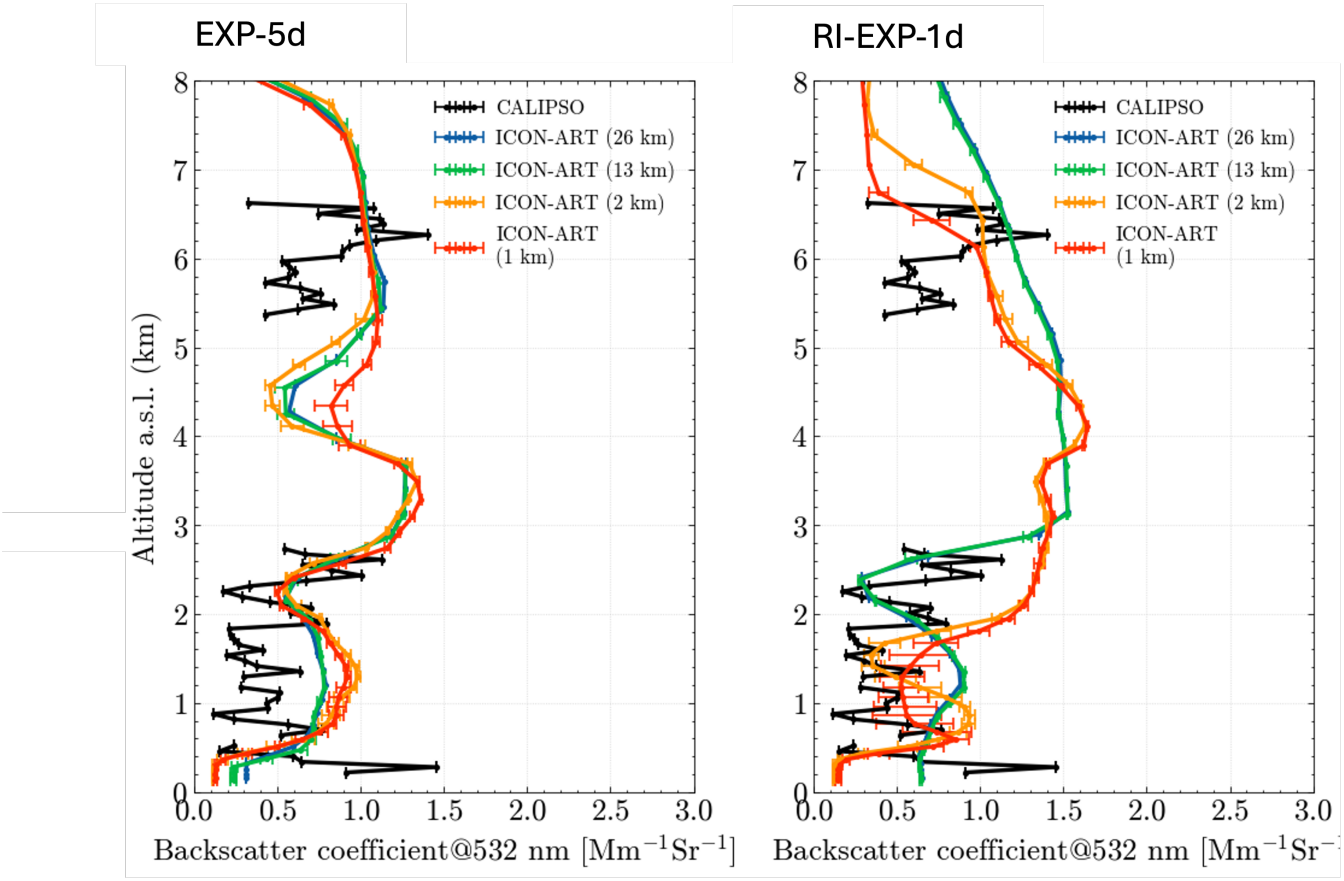


Figure S9. Vertical profiles of the aerosol backscatter coefficient from CALIPSO retrievals (532 nm) and ICON-ART simulations with different horizontal grid resolutions for EXP-5d (left) and RI-EXP-1d (right) experiments. The data was sampled at 13:00 UTC on 23 February 2021.

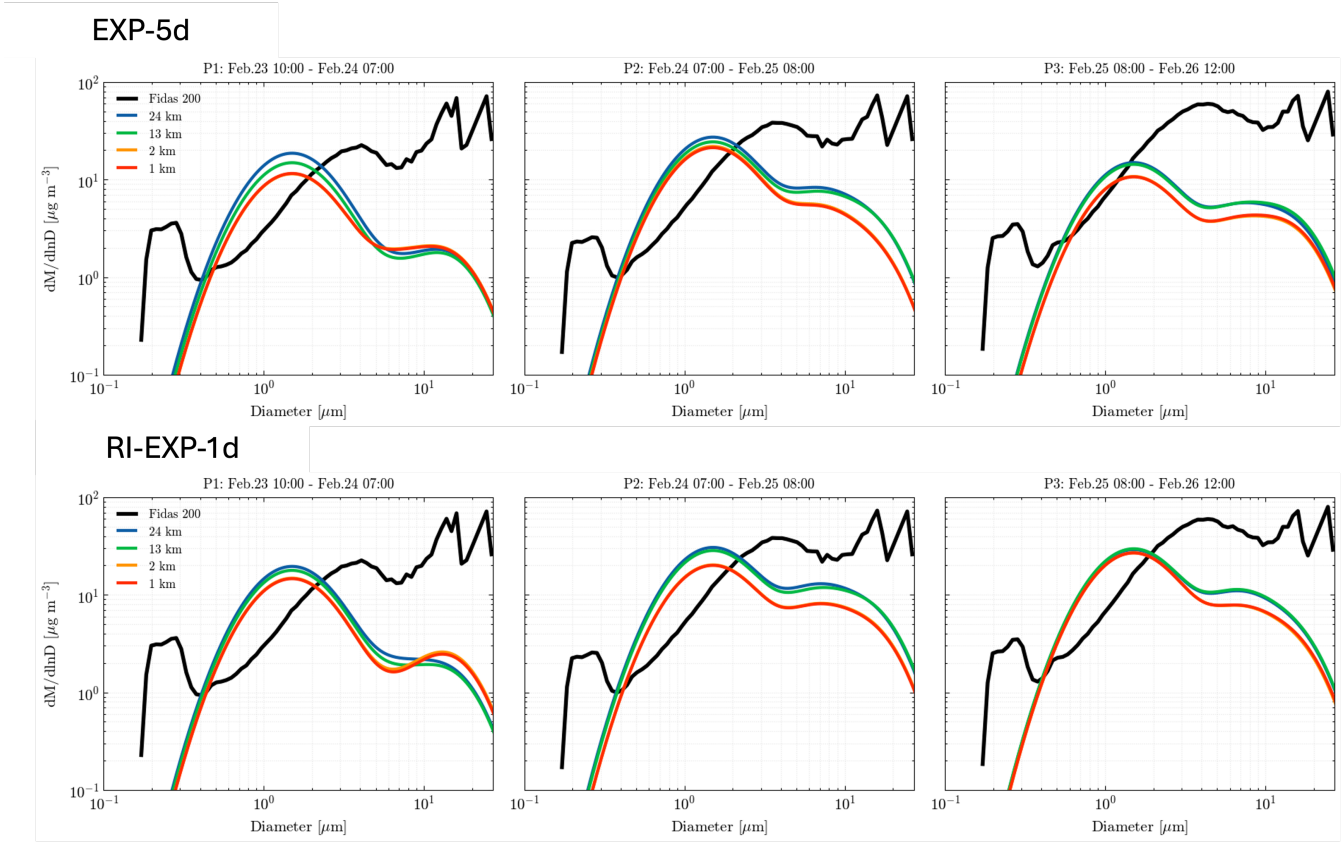


Figure S10. veraged aerosol mass size distributions (dM/dlnD) measured by the Fidas 200 optical particle spectrometer and simulated by ICON-ART for the three periods indicated in Fig. 15. Results from the continuous 5-day forecast experiment (EXP-5d) and the daily re-initialized forecast experiment (RI-EXP-1d) are shown for the Saharan dust outbreak of 21–25 February 2021.

Table S1. Normalized mean bias (NMB), root-mean-square error (RMSE), and correlation coefficient (R) of backscatter, AOD, and PM10 for different model resolutions.

Parameter	EXP_ID	Model resolution	NMB	RMSE	R
Backscatter	EXP_5d	26 km	5.92%	1.2017 Mm^{-1}	0.4110
		13 km	6.52%	1.2043 Mm^{-1}	0.3853
		2 km	6.24%	1.2214 Mm^{-1}	0.3711
		1 km	6.05%	1.2216 Mm^{-1}	0.3691
	RI_EXP_1d	26 km	50.29%	1.3301 Mm^{-1}	0.3973
		13 km	49.88%	1.3247 Mm^{-1}	0.3947
		2 km	38.40%	1.3192 Mm^{-1}	0.3714
		1 km	38.28%	1.3193 Mm^{-1}	0.3705
AOD	EXP_5d	26 km	-17.66%	0.2244	0.3122
		13 km	-16.83%	0.2165	0.3096
		2 km	-20.24%	0.2261	0.2918
		1 km	-20.25%	0.2262	0.2918
	RI_EXP_1d	26 km	23.94%	0.2588	0.3960
		13 km	24.48%	0.2574	0.4209
		2 km	17.83%	0.2556	0.4139
		1 km	17.85%	0.2556	0.4039
PM10	EXP_5d	26 km	-40.55%	23.6590 $\mu g/m^3$	0.6621
		13 km	-47.27%	24.8491 $\mu g/m^3$	0.6979
		13km	-26.5%	28.5825 $\mu g/m^3$	0.6502
		2km	-57.05%	28.6928 $\mu g/m^3$	0.6512
	RI_EXP_1d	26 km	-19.70%	14.4558 $\mu g/m^3$	0.8675
		13 km	-22.95%	14.2789 $\mu g/m^3$	0.8644
		13km	-37.58%	17.6388 $\mu g/m^3$	0.8782
		2km	-38.12%	17.8605 $\mu g/m^3$	0.8688